

Generative Adversarial Networks for Labeled Data Creation for Structural Monitoring and Damage Detection

Furkan Luleci¹; F. Necati Catbas^{1*}, Ph.D., P.E.; Onur Avci², Ph.D., P.E.

¹Department of Civil, Environmental, and Construction Engineering, University of Central Florida,
Orlando, FL, 32816, USA

²Department of Civil, Construction, and Environmental Engineering, Iowa State University, Ames, IA,
50011, USA

Abstract: There has been drastic progression in the field of Data Science in the last few decades and other disciplines have been continuously benefitting from it. Structural Health Monitoring (SHM) is one of those fields that uses Artificial Intelligence (AI) such as Machine Learning (ML) and Deep Learning (DL) algorithms for condition assessment of civil structures based on the collected data. The ML and DL methods require plenty of data for training procedures; however, in SHM, data collection from civil structures is very exhaustive; particularly getting useful data (damage associated data) can be very challenging. This paper uses 1-D Wasserstein Deep Convolutional Generative Adversarial Networks using Gradient Penalty (1-D WDCGAN-GP) for synthetic labeled vibration data generation. Then, implements structural damage detection on different levels of synthetically enhanced vibration datasets by using 1-D Deep Convolutional Neural Network (1-D DCNN). The damage detection results show that the 1-D WDCGAN-GP can be successfully utilized to tackle data scarcity in vibration-based damage diagnostics of civil structures.

Keywords: Structural Health Monitoring (SHM), Structural Damage Diagnostics, Structural Damage Detection, 1-D Deep Convolutional Neural Networks (1-D DCNN), 1-D Generative Adversarial Networks (1-D GAN), Deep Convolutional Generative Adversarial Networks (DCGAN), Wasserstein Generative Adversarial Networks with Gradient Penalty (WGAN-GP)

*Email: catbas@ucf.edu

1) Introduction and background on Structural Damage Detection (SDD)

Man-made or environmental stressors tend to decrease the remaining useful lives of civil structures. As the aging civil infrastructures are getting more vulnerable against such impacts, more comprehensive assessment and effective health management plans are needed to improve the life cycle of structures.

The typical workflow to monitor and assess an existing civil structure starts with collecting operational data with sensors such as accelerometers, strain gauges, potentiometers, fiber optic sensors or load cells. As a following step, the data is pre-processed and analyzed to perform damage identification based on the changes in the structural parameters (stiffness, mass, damping, etc.) or in the raw data to identify structural defects (crack, delamination, corrosion, bolt-loosening, spalling, etc.) The common practice of diagnosing damage in SHM is via accelerometers since it is advantageous over other methods (Catbas and Aktan, 2002; Catbas et al., 2006; Das et al., 2016).

Applications of vibration-based damage diagnostics can be divided into local methods and global methods. Local methods include Non-Destructive Testing (NDT) and some of the camera sensing techniques like Infrared Thermography (IR), Digital Image Correlation (DIC). Global methods (vibration-based) include the analysis of collected data parametrically (using physical model like FEA program or non-physical model like system identification methods) or nonparametrically (extracting meaningful features from the raw data) (Catbas et al., 2016; Avci et al., 2021). Additionally, via advanced Computer Vision methods, damage diagnostics can be performed at local and global levels (Dong et al., 2021).

Numerous studies have been reported for structural damage diagnostics of civil structures: (Gul et al., 2008) demonstrated that the boundary conditions of a structure can be determined by looking at its deflection profile which they performed the test on a laboratory grid structure. (Yin et al., 2009) detected the presence and quantified the damage by extracting the modal properties via Natural eXcitation Technique (NeXT) and Eigenvalue Realization Algorithm (ERA) from the collected vibration data of transmission towers. (Krishnan Nair et al., 2007) utilized Auto-Regressive Moving Average (ARMA) and then Gaussian Mixture Model (GMM) to first extract the features and to classify them by using Mahalanobis distance metric on the collected vibration data. They successfully identified undamaged and damaged datasets. Gul & Catbas (2011) utilized Auto Regressive eXogenous output (ARX) to extract and then clustering technique to classify the undamaged and damaged cases in the collected vibration data from a grid

structure. (Silva et al., 2016) focused on the vibration datasets to determine outliers by using Genetic Algorithm (GA) based clustering on decision boundary analysis (GADBA). One of the common details in the above-mentioned parametric and nonparametric vibration-based damage diagnostic studies is that the amount of data is not prominent on the success of the used methods.

The ML and DL methods require a lot of data samples to train the algorithms especially DL algorithms yield outstanding results on more and more data (Alom et al., 2019). With superior performance on feature extraction, classification, regression, and clustering, ML and DL methods have been widely accepted in civil SHM for both parametric and nonparametric vibration-based damage diagnostics. It is observed that Artificial Neural Networks (ANN) is the most used one in ensembled other algorithms and Support Vector Machine (SVM) comes in second for SHM applications. Some of the introduced studies are (González et al., 2008; Jungwhhee Lee et al., 2007; Cury et al., 2012; Jong Jae Lee et al., 2005; Santos et al., 2016; Bandara et al., 2014; Ghiasi et al., 2016; Abdeljaber et al., 2016). When using a ML model for nonparametric damage diagnostic purposes, features from the raw data need to be extracted (Catbas and Malekzadeh, 2016) by using some of the computational tools such as Principal Component Analysis (PCA) or Autoregressive (AR) models which causes computational complexity along with other limitations (Avci et al., 2021). On the other hand, the DL algorithms can make highly accurate predictions by learning the features directly in the raw data without having to need of any extracting tools. In other words, with correctly built model and right training process, DL algorithms can show superior performance over ML methods. In civil SHM area, few unsupervised DL methods which are mostly Autoencoders (Pathirage et al., 2018; Shang et al., 2021; Rastin et al., 2021) and some supervised DL methods which are mostly Convolutional Neural Networks (Abdeljaber et al., 2017; Yu et al., 2019; Avci et al., 2017; Abdeljaber et al., 2018) are presented.

1.2) Scope of this work

Data collection in SHM of civil structures can be exhaustive, challenging, and expensive. Requesting permission from authorities to install expensive and laborious SHM systems, requesting traffic closures, etc. and needing of skilled experts on the field are just some of the mentioned exhaustive tasks. Taking into account that only a very few civil structures have permanent SHM systems in the world, it is hard to know the damage related conditions on the remaining structures. As a result of these challenges, opportunity to find useful data (damage associated data, *labeled data*) for the civil structure is rare. This creates a class imbalance complication to implement vibration-based methods

with AI algorithms for structural assessment purposes. The effect of class imbalance on classification performance of DL model is detrimental and the impact increases when the ratio of imbalance in dataset increases. One solution can be oversampling the already existing dataset, in other words increasing the amount of dataset with exact copies of it. Yet, in this method, the AI model does not learn the variation of the damage-associated dataset but only the provided exact copies of the input which causes model to overfit. Third solution can be building a Finite Element (FE) model to produce displacement, stress, or acceleration data to tackle the data scarcity by analyzing the structure under similar damage scenarios simulated in the FE model. However, this method is not reliable compared to collecting data from a real structure as it is very difficult to simulate the damage cases comprehensively in an FE model (Gardner et al., 2019). These challenges can facilitate inaccurate results for DL models when used for vibration-based damage diagnostics.

While the data scarcity hinders the utilization of the ML and DL algorithms, the study presented in this paper introduces the state-of-the-art Generative Adversarial Networks (**GAN**) in structural damage diagnostics. The GAN is utilized to generate data samples to train the Deep Convolutional Neural Network (**DCNN**) to perform nonparametric vibration-based damage diagnostics on a laboratory structure. The scope of the presented work is a good fit for representing realistic scenarios that could be encountered during the operational lives of civil structures. For instance, when the existing dataset is very scarce to run a DL model to perform damage detection, GAN can be employed to enhance the training datasets with synthetic samples of data. The introduced methodology in this paper will pave the way for additional ML and DL algorithms to be integrated in the damage diagnostics on civil structures.

1.3) Existing work on Generative Adversarial Networks

(Ian J. Goodfellow et al., 2014) proposed a semi-supervised DL network which contains two distinct networks: a generative network, G_θ , that captures the given randomly distributed data, z , and aims to maximize the probability of the output it generates, $G_\theta(z)$, very alike to the training dataset, x , in other words, generator tries to minimize the probability that prediction of discriminator on generator's outputs are not real. The discriminative network, D_ϕ , aims to maximize the likeliness of the output it gets from the generator, $G_\theta(z)$, is not real and from the training data, x , is real. Thus, it is thought as a two-player game where each player is trying to trick each other. The fundamental formulation of loss function of GAN is shown in Equation 1.

$$\min_{\theta} \max_{\varphi} V(G_{\theta}, D_{\varphi}) = \mathbb{E}_{x \sim p_{data}(x)} [\log D_{\varphi}(x)] + \mathbb{E}_{z \sim p_z(z)} [\log(1 - D_{\varphi}(G_{\theta}(z)))] \quad (1)$$

The GAN is successfully used on image-based applications and then adopted in several other applications. Among all the DL networks, GAN training is arguably the most difficult one. For example, reaching a convergence due to the difficulty of finding a unique solution to Nash equilibrium where the model is searching for a balance point between the two sides in the optimization, instead of finding a minimum one. Consequently, GANs experience large oscillations in loss values which leads to unstable training process and model performance. Occasionally, GANs suffer from mode collapse, in another words, the generator learns only some specific features in the given training data where the discriminator can be deceived. Thus, the GAN keeps producing the same data samples to trick the discriminator which reduces the creativity of the model and diversity of the outputs. GANs also suffer from the discriminator being powerful over the generator. As a result, training the generator could fail due to vanishing gradients, hence, the discriminator does not provide enough information for generator to learn (Ian Goodfellow, 2016; Salimans et al., 2016). Some tips namely “hacks” are introduced in the DL community to alleviate these drawbacks, and some of which are used in the presented work herein.

(Radford et al., 2015) introduced the use of convolutions in GAN (and called it **DCGAN**) after their successful adoption in computer vision applications. They noted that convolutions helped GAN to learn significantly better. However, to address the challenges in training of GANs, (Arjovsky et al., 2017) introduced GAN that uses Wasserstein distance as a loss function (**Wasserstein Generative Adversarial Networks - WGAN**) and demonstrated that it improves the training remarkably. In WGAN, they used “critic” over discriminator where instead of scoring the likelihood of the generated data is real or fake, it scores the output of generator as how close to the real or fake on a given image. Essentially, WGAN looks for a minimization of the distance between the produced and the training dataset distributions in the range of a real or fake distance. GAN benefited greatly from using Wasserstein metric. It provided more stable training; the results are less sensitive to the parameters and model architecture; and the loss function is more meaningful which directly relates to the quality of generated images. WGAN uses weight clipping to enforce the Lipschitz constraint on the critic to compute the Wasserstein distance; however, it causes the model to lower its learning capacity. It is also very sensitive to the selected parameters. If large weight clipping is used, it increases the computation time drastically; if the clipping is small, it could easily lead to vanishing gradients. To tackle the weight clipping problem, (Gulrajani et al., 2017) proposed a penalization of the gradient during the training of the

critic instead of using weight clipping. They showed that the method they introduced yields better performance than WGAN and resulted in more stable training and they named presented the model as **WGAN-GP (Wasserstein Generative Adversarial Networks using Gradient Penalty)**.

Computer Vision field largely benefited from using GANs on various image applications which are 2-D data. Additionally, some studies in different disciplines were successful at using GANs for 1-D data generation and data reconstruction for various purposes (Truong et al., 2019; Kuo et al., 2020; Luo et al., 2020; Wulan et al., 2020; Tiantong Wang et al., 2021; Sabir et al., 2021). Several GAN based 1-D data generation, reconstruction, and ML classifier related studies are presented in field of non-civil SHM (Shao et al., 2019; Guo et al., 2020; Gao et al., 2019; Xuewen Zhang et al., 2021). In the civil SHM field, few studies are presented for GAN based 1-D data reconstruction (Chi Zhang et al., 2018; Jiang et al., 2021; Fan et al., 2021). Yet, at the time of this paper preparation, there was not any study utilizing the **WGAN** and **WGAN-GP** comprehensively to address the data scarcity issue for civil SHM, to the best information of the authors.

2) Framework of the study

In the proposed work, **1-D WGAN-GP** that is built on convolutions is used to generate synthetic datasets which is named as “**1-D WDCGAN-GP**” in short by the authors for **One Dimensional Wasserstein Deep Convolutional Generative Adversarial Networks using Gradient Penalty**. Then, 1-D DCNN (**1-D Deep Convolutional Neural Network**) is used to implement nonparametric damage detection on the scenarios that might be encountered during an SHM of civil structures. For simplicity, in the remaining of the paper, **1-D WDCGAN-GP** and **1-D DCNN** is referred to as M_1 and M_2 , respectively. The rest of the paper is presented in the following order: framework of the study in section 2, workflow of the 1-D WDCGAN-GP in section 3, and workflow of the 1-D DCNN in section 4. Summary and conclusions are presented at the end.

The vibration dataset used in this work is obtained from a study by (Abdeljaber et al., 2017; Avci et al., 2022) on a steel laboratory frame (Fig. 1) where they installed 30 accelerometers at 30 joints. A modal shaker excitation is applied to the structure and consequently 1 undamaged and 30 damaged scenarios are created at each joint separately by loosening the bolts at the steel connections between filler beams and girders. Then, at a 1024 Hz of sampling rate, they collected 256 seconds of vibration data with a total sample of $256 \times 1024 = 262,144$ from each accelerometer

channel dedicated to a joint (Fig. 1). The 1-D vibration arrays are named as **tensors** and notation used in this paper is $n[a_{klf}]_s$ where k represents the condition such as **0** refers the data is collected in an **undamaged scenario**, **1** refers the **damaged scenario**, l represents the **joint number (only joint 1 is used in this study)** where the data is collected from based on Fig. 1, and f refers to “**fake**” if the tensor is generated by the M_1 . Lastly the s and n refer to **number of samples** that each tensor contains and **number of tensors**, respectively. The n is featured to 1, if there is no number written.

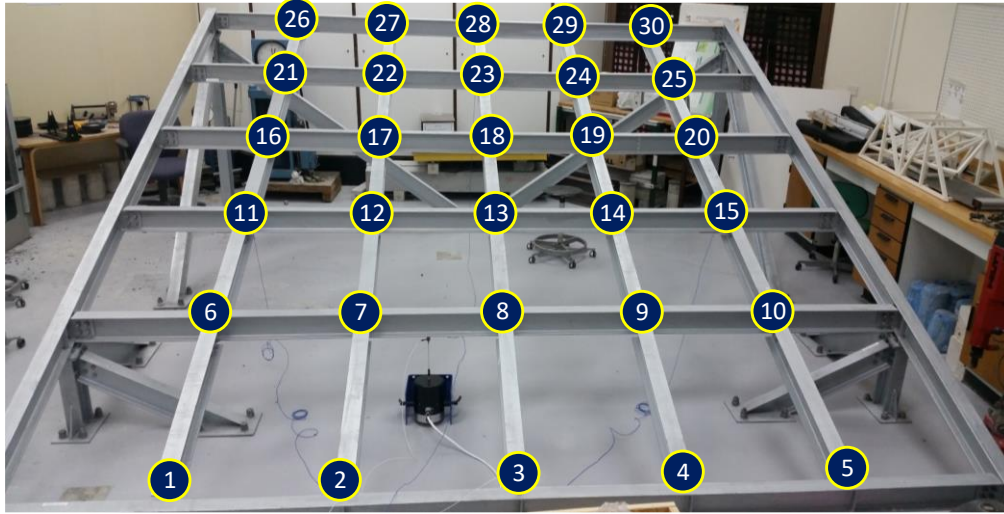


Fig. 1. Steel Frame Grand Simulator Structure (Abdeljaber et al., 2017)

Only two different sample sizes are used in this study: 1024 and 262,144. To represent the sizes of samples in a simple way, they are denoted as r and b respectively where r refers to “**raw**” and b refers to “**batch**”. The M_1 generates data that has 1024 samples which is also the used batch size in the M_1 . In order for M_2 to use the training (raw or r) tensors and generated (batch or b) tensors together, 1024 sizes of tensors are also created by batching randomly from the one single 262,144 vibration dataset which is $[a_{11}]_r$. Note that the produced tensors from the M_1 are also generated randomly because the input, $[a_{11}]_r$ of M_1 is batched sampled in shuffle mode during the training. Two reason why batching in shuffle mode are used is: (i) to prevent the any bias in the model such as learning the data in the order that is provided and (ii) to converge the training faster. A similar method is also successfully implemented and described by (Abdeljaber et al., 2017). They divided the input signal into frames and randomly shuffled it. Nevertheless, the sequence of the dataset or the parameters of the vibration tensors are irrelevant because the purpose of the study is to show that GANs can tackle the data scarcity for nonparametric damage diagnostics for civil structures. Lastly, the PC

used in this study has the following specs: 16 GB RAM DD4 2933 MHz and NVIDIA GeForce RTX 3070 8GB GDDR6 graphic card.

The workflow of this study is presented in Fig. 2. First, the tensor $[a_{11}]_b$ is inputted in the M_1 to generate the synthetic datasets of $[a_{11f}]_b$. Then, the $[a_{01}]_b$ and $[a_{11}]_b$ are extracted to the data pool. Subsequently, these tensors are used in M_2 as 4:1 ratio for training and testing data for six different scenarios which five of them includes potential real-life cases. In Scenario#0, for benchmarking purposes with other scenarios, no synthetic data involved in, but only real tensors are used. To represent that, $60[a_{01}]_b$ and $60[a_{11}]_b$ for training and $15[a_{01}]_b$ and $15[a_{11}]_b$ tensors are used for testing. In Scenario#1 to Scenario#5, real undamaged tensors are used for both training and testing; however, for each scenario, a different amount of synthetic tensor enhancements implemented for damaged datasets along with the real ones for training and testing. To represent the $60[a_{01}]_b$ and gradually changing dataset sizes of $[a_{11}]_b$ from 10 to 50 and along with gradually changing dataset sizes of $[a_{11f}]_b$ from 50 to 10 for training as shown in Fig. 2. For testing $15[a_{01}]_b$ and $15[a_{11}]_b$ tensors are used. The reasoning behind of creating the scenarios in this way is to reflect the possible scenarios that can be encountered in SHM to perform damage diagnostics of civil structures. As previously mentioned, obtaining damage-associated dataset from large civil engineering structures is challenging; and to do damage diagnostics via DL model on a particular structure, it is essential to have sufficient amount of data samples for each class (undamaged or damaged classes).

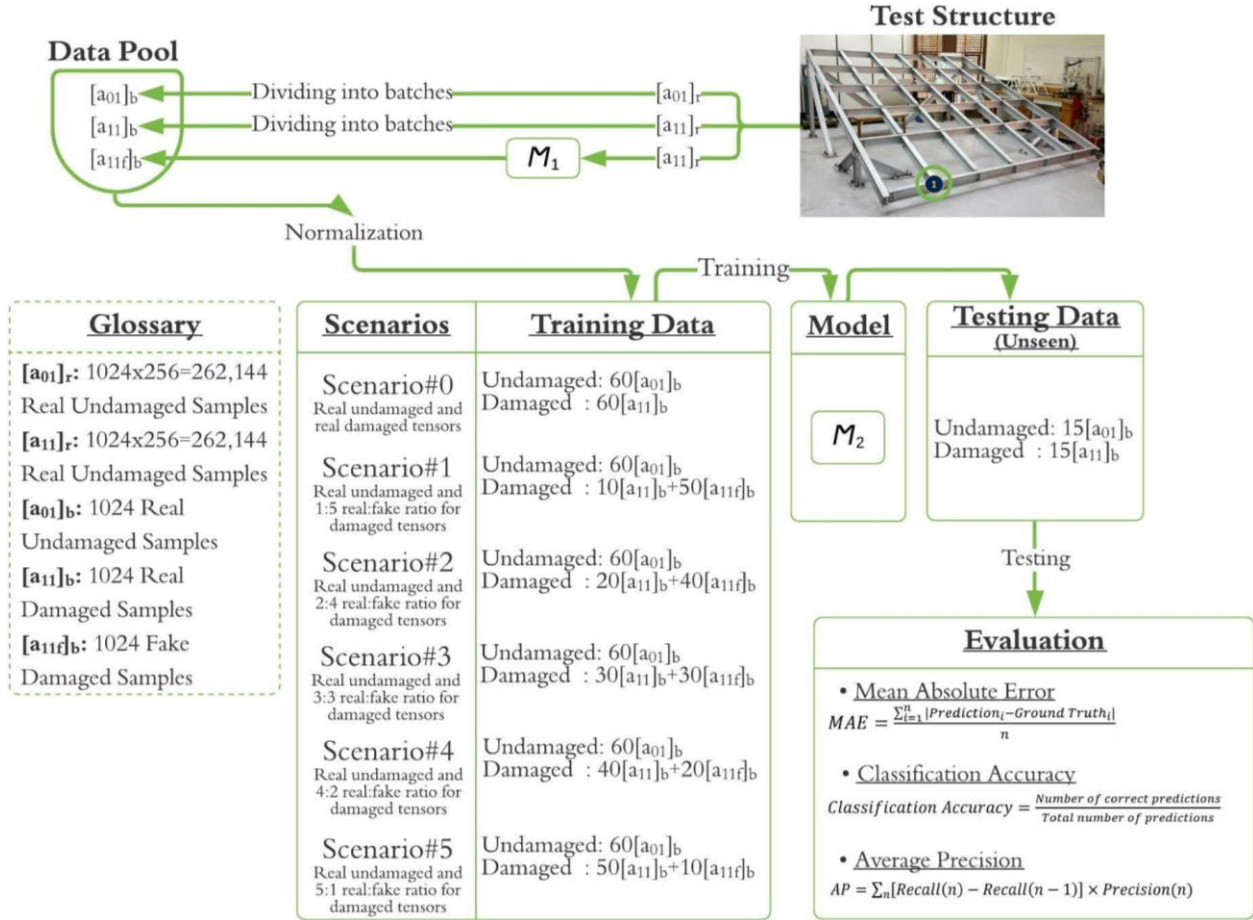


Fig. 2. The framework

Each scenario presented in Fig. 2, from Scenario#1 to Scenario#5, shows that an enough amount of undamaged dataset exists, but the sample in the damaged dataset is very scarce for a particular damage case. This could be associated to a delamination in the girder of a multi-span bridge. For instance, single channel vibration datasets were previously collected on the first 6 spans (among 18 spans) of a bridge. It is previously known that the first 5 spans contain undamaged, and the 6th span contains damage features in the dataset. To diagnose the conditions of remaining 12 spans via a DL model (that might potentially house similar types of damage), it is prominent to have a trained DL model on that damage-associated dataset. Yet, under given circumstances, the dataset suffers from class imbalance due to data scarcity (5 undamaged and 1 damaged datasets among a total of 6 datasets corresponding to 6 spans). To tackle this problem, GANs can be used to generate synthetic (artificial) data for the DL model to be trained effectively. This instance is illustrated in Fig. 3 and Fig. 4. Fig. 3 illustrates the vibration-based damage diagnostics via DL model. Fig. 4 illustrates the GAN enhanced vibration-based damage diagnostics via DL model. In fact, the Scenario#1 to

Scenario#5 shown in Fig. 2 describe enhancing the real damaged data with different ratios of synthetic damaged data. With different scenarios introduced in Fig. 2, it is intended to demonstrate the effect of the enhancement in the training dataset and the subsequent impact on the prediction results by the M_2 . Next sections explain the M_1 and M_2 workflows are explained in the next sections.

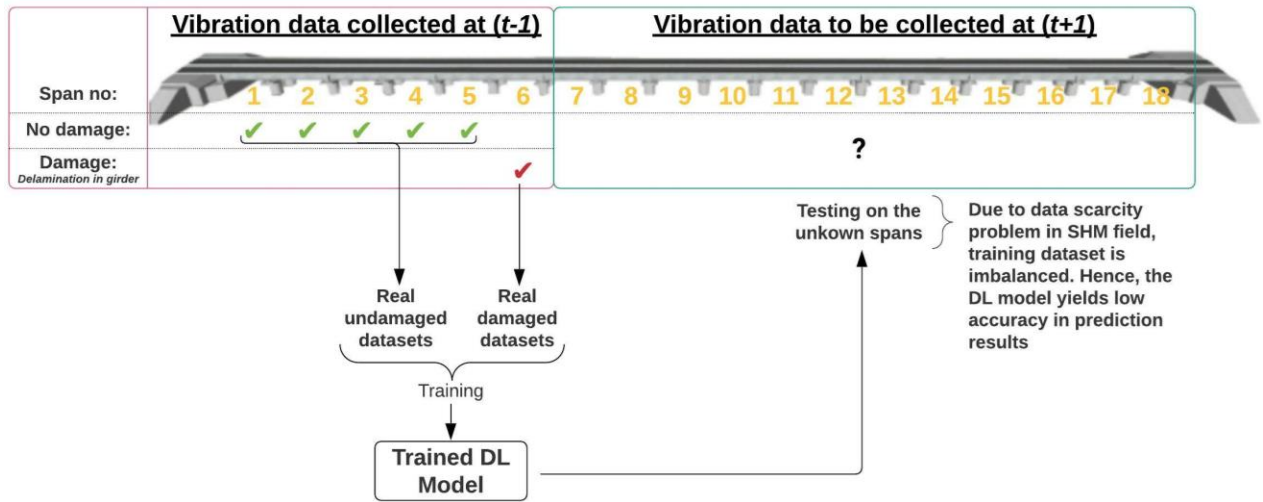


Fig. 3. Vibration-based damage diagnostics via DL model

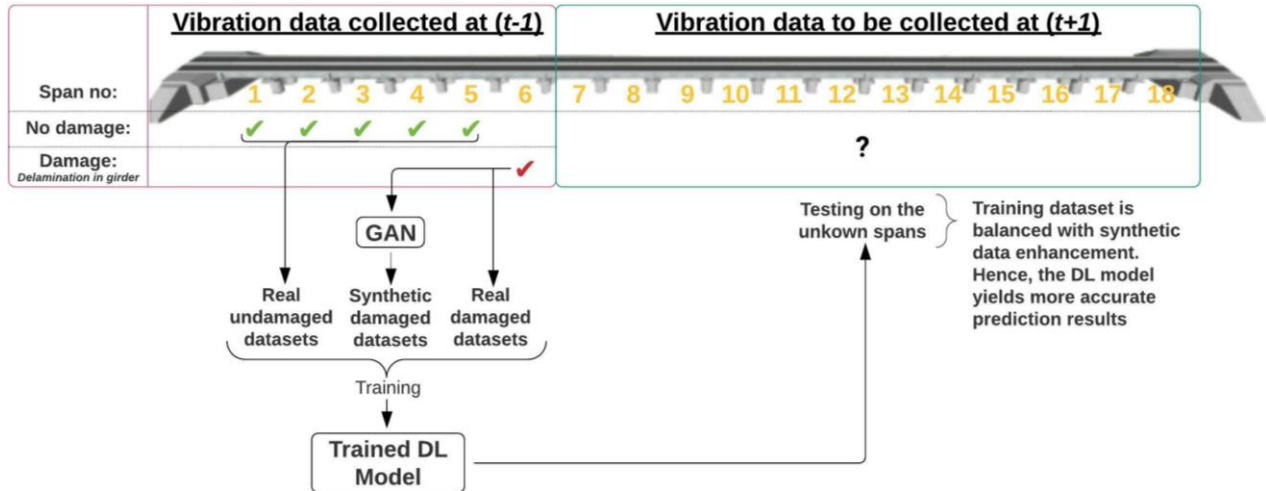


Fig. 4. GAN enhanced vibration-based damage diagnostics via DL model

3) Workflow of 1-D WDCGAN-GP (M_1)

3.1) M_1 - data preprocessing

Before the DL model training, the standard practice in the DL field is to normalize the inputs in the same scale. Thus, model can learn and predict more efficiently. During the model training, normalizing helps with the weights to be at the same scale. In other words, during the front and back propagation through the network where the dot products of the weights are computed, the normalization assist the model to perform accurate results and decrease processing time. In case the dataset has spikes, the normalization would help, otherwise the spikes have a significant impact on the propagation because different levels of weight calculations can negatively affect the model quality during training. Yet the dataset, $[a_{11}]_r$, does not possess large spikes. Also, the M_1 consists of layers of batch and instance normalization which normalize the sampled batches during training. After a training session of M_1 with normalized input and unnormalized inputs, the results seem that they are not distinctly different. In fact, it is believed that when the model is fed with the unnormalized data, it captures the spatial-temporal features in the dataset more effectively. Thus, normalization is not carried before using the inputs for the M_2 .

3.2) M_1 – architecture

As a primary step, different options of layers and parameters are used in the architecture and the one with the best performance is selected. The used model architecture is illustrated in Fig. 5. The architecture takes the randomly given noise tensor (z) and passes it through the five 1-D transpose convolutions. The first layer is $filter = 64, stride = 2, padding = 0$, then the rest of the layers are $filter = 4, stride = 2, padding = 1$. The batch normalization and ReLU is used after every layer except the last one. At the end of the generator part, Tanh activation function is used and consequently, $[a_{11f}]_b$ is created. Then, $[a_{11}]_b$ and $[a_{11f}]_b$ are passed to the critic (the “discriminator” is named in WGAN “critic” as in their original paper) to be scored by the critic as to how real or fake each passed tensor is. Then the tensor passes through five 1-D convolutions. The first four layers are $filter = 4, stride = 2, padding = 1$ and the layer is $filter = 64, stride = 2, padding = 0$. Leaky ReLU and dropout is used after the first layer. For the rest, instance normalization along with ReLU is used at the end of each layer.

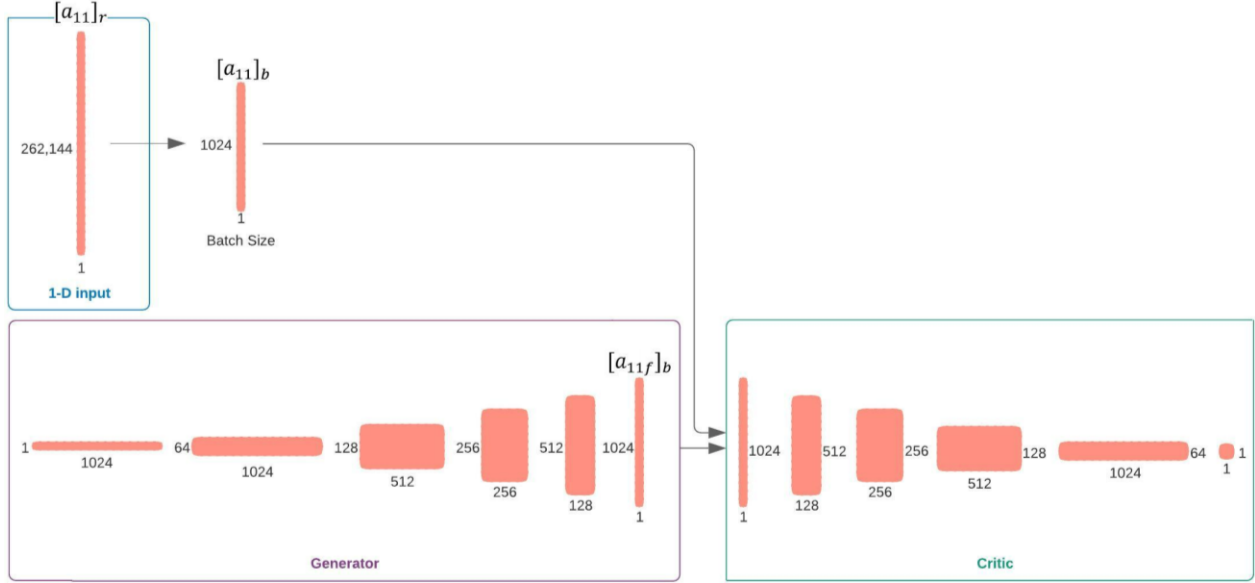


Fig. 5. 1-D WDCGAN-GP (M_1) Architecture

3.3) M_1 - training and fine tuning

As previously mentioned, the training phase of GANs is the most challenging part and they are known in the DL community as hardest model to train. Thus, it needs substantial effort during fine-tuning process. Even though the model used in this paper is one of the most advanced GAN model, 1-D WDCGAN-GP, few approaches (so called hacks) have taken for the fine-tuning. After plenty of trials with different parameters in the model, using one layer of dropout with 70% in the critic is found very beneficial which avoids the overfitting and reduces the capacity of the critic and helps the model to reach the Nash equilibrium. Moreover, a random Gaussian noise is added that decays over each epoch (iteration). Thus, it gives handicap to the critic not to be superior to the generator. Consequently, the learning rate of 5×10^{-6} for generator and 2×10^{-5} for critic yielded the best result. The critic iterations, lambda parameter for the gradient penalty, and batch size are respectively picked as 12, 20, and 1024. The epoch number is used as 600 and took 44 hours of training. The AdamW optimizer is used in both the generator and critic for the optimization process. Lastly, the generator and critic loss functions are seemed to be converged at zero axis (Fig. 6) which is explained detailly in the next section.

3.4) M_1 - evaluation and interpretation

As training GANs are arguably the hardest ones among other DL models, evaluation of them could be very challenging as well. Unlike the other DL models, GANs do not have objective function which makes it harder to evaluate the performance of the model. The evaluation of the GANs can be categorized as qualitative (manual evaluation) and quantitative where the former is based on visual, and the latter is based on numerical evaluation. The widely used form of evaluation methods of GANs is qualitative approach that is visually evaluating the outputs of the generator in comparison with the training data; and the data is mostly in the form of images. However, this approach suffers from some drawbacks such as limited number of generated output can be viewed at a time by an observer and subjectivity is introduced from observers. Additionally, implementing this approach is not as effective as doing it on 1-D signal data. Therefore, several quantitative evaluation metrics are introduced to evaluate the performance of the model with no reached consensus in the DL as to which metric is the most effective. In a study by Borji (2018) the evaluation methods of GANs are investigated. One of the most used metric for evaluating GANs is the Fréchet Inception Distance (FID) score (Heusel et al., 2017) which is introduced as an improvement over Inception Score (IS) which is reported to be unable to capture the distribution of real and generated output. Also, several comparative studies proved its effectiveness against other GAN evaluation metrics. Particularly, FID showed very consistent performance when compared to manual evaluation of the GAN outputs. The formula of FID is based on a statistical formulation that is shown in Equation 2.

$$FID(x, g) = \|\mu_x - \mu_g\|_2^2 + Tr(C_x + C_g - 2(C_x C_g)^{0.5}) \quad (2)$$

Where respectively the μ_x and μ_y are the means and C_x and C_g are the covariance matrices of real and generated signals and Tr is the trace of the matrices e.g., the sum of all the diagonal elements in the matrices. The lower the FID score, the more similar the compared data.

Another quantitative evaluation metric is introduced by Guan et al. (2019) where the performance of GAN is evaluated on images based on three aspects: **Creativity**, **Inheritance**, and **Diversity**. These aspects are very significant for evaluating the GANs as they are expected to add creativity and diversity in the outputs as well as to keep the inheritance of the real input (Guan et al., 2020). Among three, the Inheritance aspect is generally used for images where it shows how the generated images retain the key features of the real images such as texture. Therefore, it is not used in this presented study. The Creativity aspect indicates to what extent the generated outputs are not the exact

ones of the real outputs (or dissimilar to each other) and the Diversity aspect indicates to what extent the generated outputs similar to each other. The Creativity and Diversity computations are carried out by using Structural Similarity Index Measure (SSIM) (Z. Wang et al., 2004) which was first used for image quality assessments by using similarity between the pixels of two images. If the SSIM of two images is 1, they are exactly same; if the SSIM is 0, then they are entirely different images. The authors of the paper (Guan et al., 2019) defined a threshold value of 0.8 to calculate the creativity index; for instance, if the SSIM of generated and real data are higher than 0.8, they are concluded as duplicates. No threshold is used for the diversity index, but SSIM is employed between the generated datasets to compute the index. There is no consensus on what SSIM values or thresholds should be used for creativity and diversity approaches for evaluation of GANs. Intuitively, calculating SSIM of the generated outputs to real inputs indicates how creative the outputs are from the inputs. Calculating SSIM of the generated outputs to each other in the generated output dataset gives how diverse the outputs from each other in range of 0 between 1. The Creativity and Diversity indices are not directly used in this study, but SSIM computation is carried out to evaluate the extent of creativity and diversity of the generated outputs. As a result, in this study, the creativity approach is investigated by computing SSIM between the generated and real tensors; the diversity approach is investigated by computing SSIM between the generated tensors within the generated dataset from the M_1 . The SSIM equation is:

$$SSIM(x, g) = \frac{(2\mu_x\mu_g+c_1)(2\sigma_{xg}+c_2)}{(\mu_x^2+\mu_g^2+c_1)(\sigma_x^2+\sigma_g^2+c_2)} \quad (3)$$

In Equation (3) μ_x and μ_g are the means, σ_x and σ_g are the standard deviations, and σ_{xg} is the covariance of real data (x) and generated data (g). The c_1 and c_2 are the constants which are multiplication of k_1 and L ; and k_2 and L respectively, to stabilize the division with weak denominator. L is the dynamic range of the signal and k_1 and k_2 are the constants which are picked in this study as 1×10^{-2} and 3×10^{-2} .

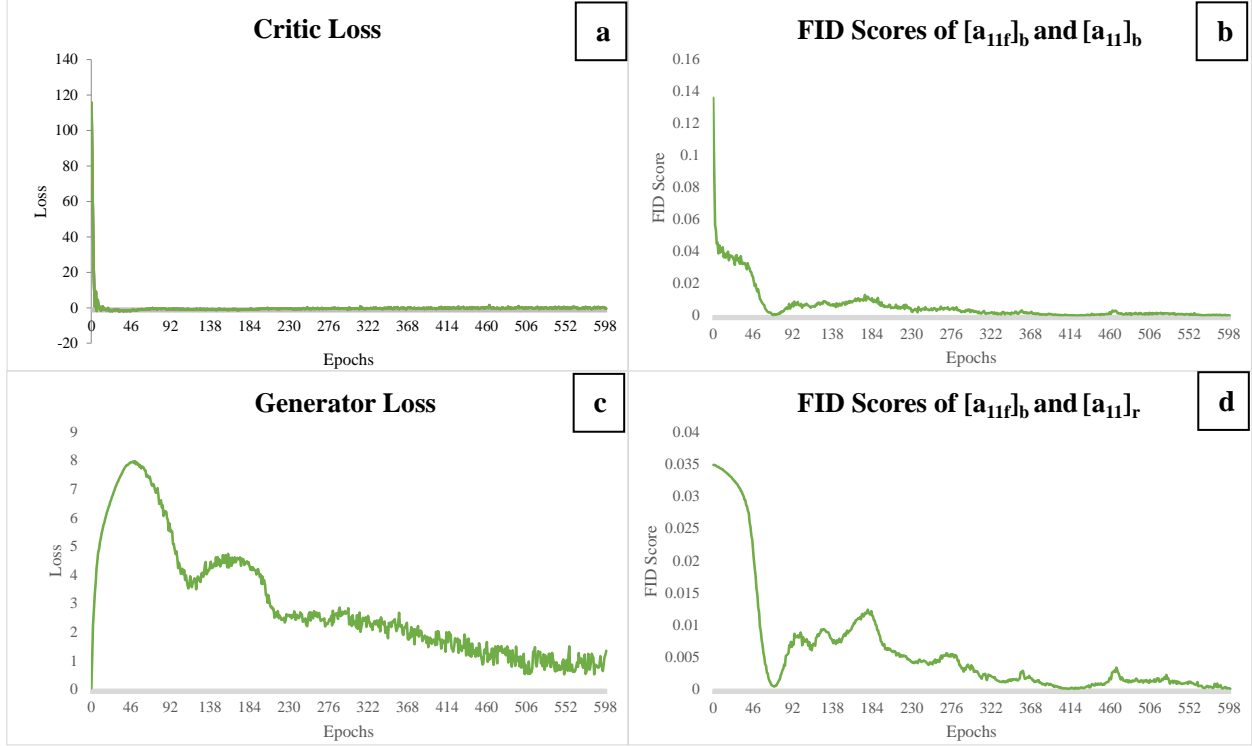


Fig. 6. Training plots of 1-D WDCGAN-GP (M_1)

During the training, the critic loss, the generator loss, and FID scores are monitored to observe the performance of the model (Fig. 6). It is noted that the critic loss converges to zero. The generator loss first increases since the critic has more knowledge on the real data domain and can easily guess the generated outputs; yet, after some epochs, generator starts learning the gradients and generate more similar datasets. Hence, the generator loss seems to be returning to its first loss values which is expected for WDCGAN-GPs. The FID scores are monitored by computing the tensors between $[a_{11f}]_b$ and $[a_{11}]_b$ and they appear to be converging to zero. In other words, they are getting look alike to each other (Fig. 6b and 6d). It is also important to note that the generated outputs, $[a_{11f}]_b$, are not only becoming similar to batched real data, $[a_{11}]_b$, but also to the entire raw signal data, $[a_{11}]_r$. The FID between $[a_{11f}]_b$ and $[a_{11}]_r$ is calculated during the training. It is found that the FID scores of $[a_{11f}]_b$ and $[a_{11}]_b$ and the FID scores of $[a_{11f}]_b$ and $[a_{11}]_r$ are both converging to zero with the same trend over the epochs. This reveals that batch sampling from the raw data, $[a_{11}]_r$, in shuffle mode, does not produce different results since the 262,144 sized raw dataset have repetitive features in particular time length. Hence, it validates using the batch samples of 1-second tensors (1024 samples in each tensor) in this study. Note that since the aim of this study is nonparametric damage diagnostics, that is not based

on any parameters but directly on raw data, the order of the samples in the batch sampled tensors is irrelevant. Batch sampling in shuffle mode also helps the training of the model in a way that it converges faster, preventing bias, and preventing learning the order of the data. Therefore, for simplicity, in the rest of the study, only the calculations between batch sampled generated and real datasets ($[a_{11f}]_b$ and $[a_{11}]_b$) are considered. Furthermore, in Fig. 6, it is observed that the FID score of $[a_{11f}]_b$ between $[a_{11}]_b$ are started from 0.136 and decreased to 1.5×10^{-5} , which is a reduction of 9060 times. This large reduction shows that the model learned the dataset thoroughly and can generate very similar datasets. The FID scores can depend on various factors (model architecture and hyperparameters and used dataset) as to how much it reduced, or where it started and ended. To better comprehend the FID values, in one study by (Costa et al., 2019), the authors compared their GAN model to others on MNIST data (image dataset of handwritten numbers) and the FID score was decreased by 6 times during the training. In another study, the resulted decrease in FID score was found around 85 (MITCSAIL, 2019). Although a decrement of 9060 times can be looking like a success, it might also be an indication of overfitting which will be investigated in the following paragraph.

After the M_1 is trained, the FID scores are computed between the real and generated tensors, $[a_{11}]_b$ and $[a_{11f}]_b$. Then, the Probability Density Function (PDF) is plotted of the calculated FID scores (Fig. 5). It is seen that the FID scores are dense around the value of 7×10^{-4} . The purpose of visualizing the PDF is to comprehend the variance of FID values. Although during the training it went down to 1.5×10^{-5} , the variance of the FID scores could have been extending to a value of 0.10 as well, which in this case it could be concluded that model did not learn. However, as

seen in the Fig. 7, the variance is considerably low along with very low FID values, 194 times lower than the starting point of 0.1359.

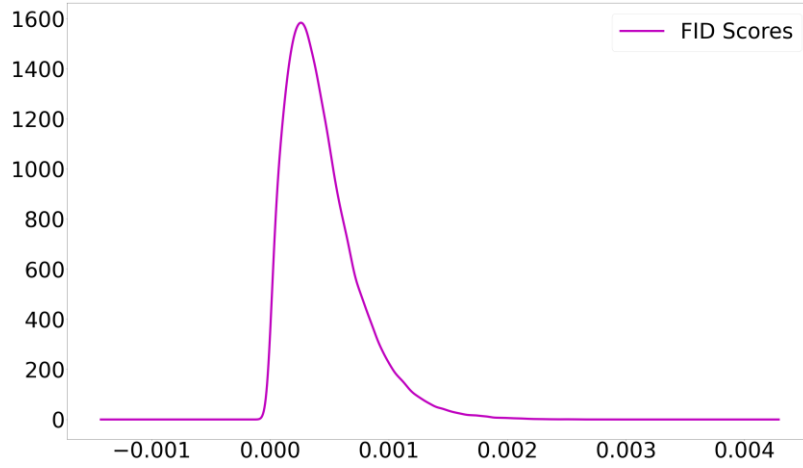


Fig. 7. Probability Density Function plot of FID Scores

Next, the creativity and diversity approaches are investigated. For that, the SSIM between the $[a_{11f}]_b$ and $[a_{11}]_b$, and SSIM within the $[a_{11f}]_b$ are computed respectively. The PDFs of the creativity and diversity results are plotted in Fig. 8. The SSIM values do not go beyond 0.8 threshold value and they are dense around the value of 0.3 which can be concluded that the generated tensors are not the exact copies of the real tensors. Thus, M_1 can generate creative outputs. The creativity measure also determines the overfitting of the model; considering that the resulted value is small, it can be concluded that the model is not overfitted in the training dataset since no exact copies exist. The diversity values are dense around the value of 0.36 and it can be stated that the generated tensors are not alike to each other. This can mean that a diversity exists within the generated tensors. Based on the creativity and diversity aspects of the generated dataset, none of the generated and real tensors are the exact copies of each other and none of the generated tensors are exact copies of each other.

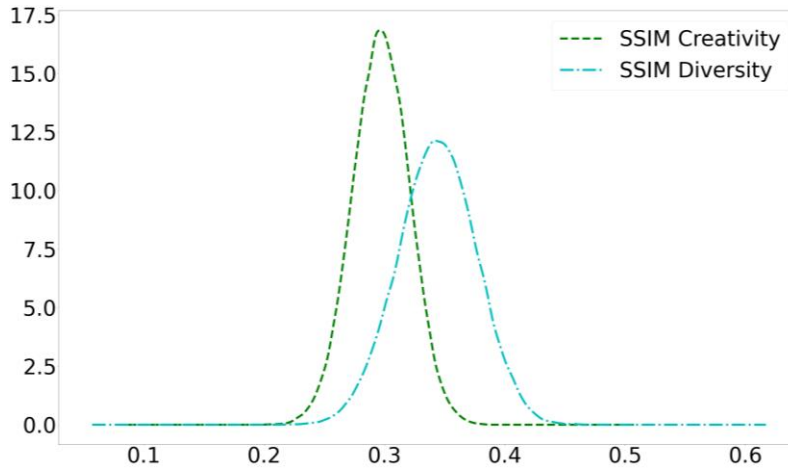


Fig. 8. Probability Density Function plots of Creativity and Diversity by using SSIM

A two pair of vibration tensors two from real and two from generated dataset are box plotted in Fig. 9 to visualize and compare the statistical meanings. The plotted tensors are picked as one pair has the lowest FID, and one pair has the lowest FID score. The boundaries of boxes and size of whiskers are looking alike along with the mean and median values. The box plots show that the statistical meanings and distributions of the generated and real data pairs are very similar to each other.

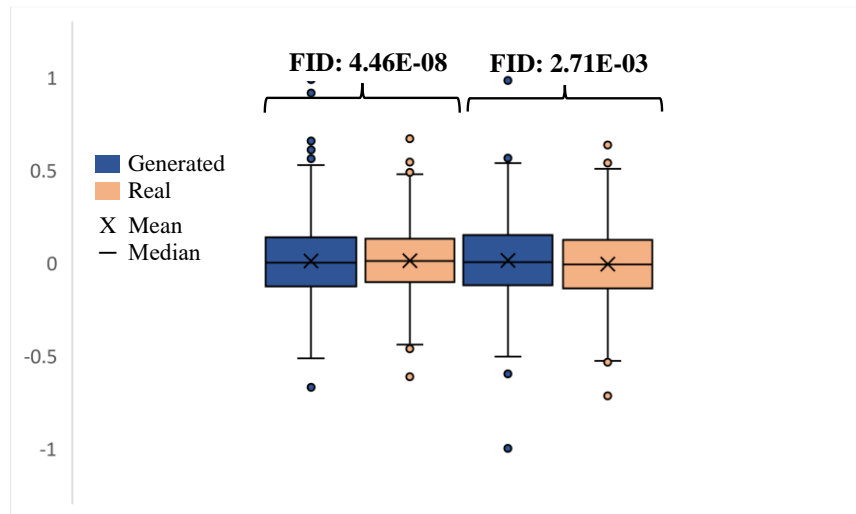


Fig. 9. Box plots of the tensors with lowest and highest FID values

Lastly, qualitative evaluation is implemented on the real input and generated outputs of M_1 . As previously mentioned, qualitative evaluation is the most preferred method for image data, 2-D data, yet it has drawbacks for evaluating 1-D

data. The same vibration tensors that were used in Fig. 9 are plotted in Fig. 10. Although it is difficult to determine the similarity between the generated and the real data as in image-based applications, the plotted tensor pairs in Fig. 10 reveal good consistency throughout the sample length for the lowest and highest FID score ones.



Fig. 10. Tensor pairs with lowest and highest FID values

4) Workflow of 1-D DCNN (M_2)

4.1) M_2 - data processing

Before feeding the tensors in the M_2 (1-D DCNN), the tensors are normalized in the range of -1 and +1. Subsequently, the generated tensors from M_1 and batch sampled tensors from the $[a_{11}]_r$ are randomly extracted into the data pool. Then, the datasets are arranged to be used for each different scenarios as stated in Fig. 2.

4.2) M_2 - architecture

The same critic architecture used in M_1 is utilized for M_2 with adding a sigmoid function at the end of the M_2 in order to produce a prediction score for each tensor (the critic network in M_1 had no activation function at the end of the last layer and only realness or fakeness scores were processed). The sigmoid function produces prediction scores in range of 0 to 1 where 0 denotes undamaged and 1 denotes damaged tensor. Lastly, unlike in the critic network of M_1 , no dropout is used in M_2 since it is not considered as necessary for a simple detection process.

4.3. M_2 – training and fine tuning

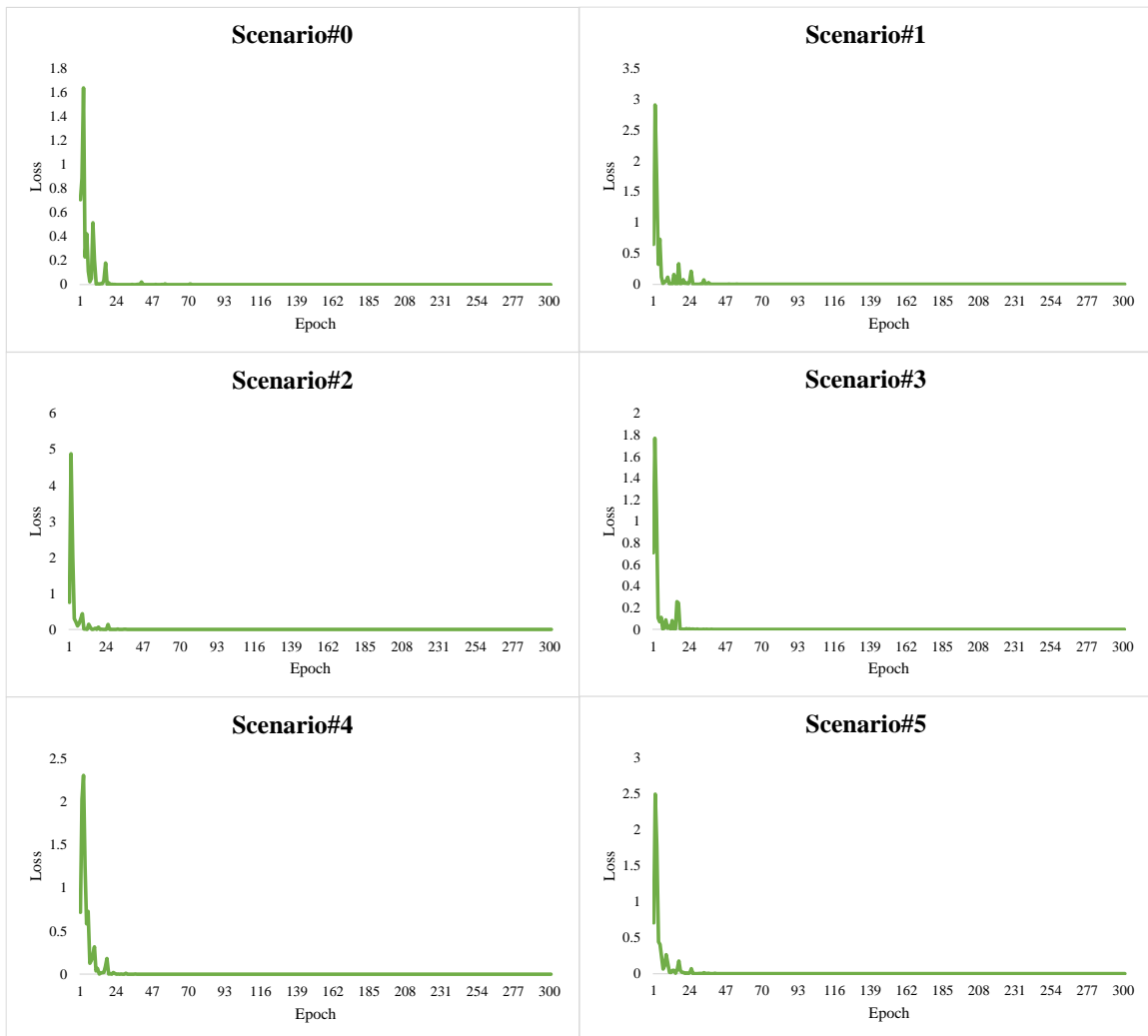


Fig. 11. Training plots of M_2 (1-D DCNN) for each scenario

After several trials of using different hyperparameters in the M_2 , the learning rate for the Scenario#0, Scenario#1, and Scenario#2 are chosen as 8×10^{-4} and for the rest of the scenarios it is 3.5×10^{-3} . The batch size and number of epoch is picked as 30 and 300, respectively. Also, Cross Entropy is used as the loss function which was not used in M_1 . Finally, the training loss functions are plotted in Fig. 11 which is seemed to be converged at zero axis for all scenarios, in other words model learned the training dataset. Then, the model is tested on the unseen tensors for each scenario and yielded successful results which is explained in detail in the following section.

4.4) M_2 - evaluation and interpretation

Regardless of how the model learned the training dataset successfully, the testing phase determines the performance of the model (testing dataset contains instances that the model did not see before, in other words *unseen* data instances). Additionally, the success of the model on the unseen data indicates if the model is overfitted to the training data and cannot generalize to other datasets.

The test results are evaluated by using one regression two classification metrics. The reason why a regression metric used on a classification problem is to measure the error on faulty predictions. In a simple vibration-based damage detection problem in SHM, a prediction score such as 0.77 can be both interpreted as damaged data (with a threshold assumption of 0.5 and converting into label of “1” which indicates damage data) and the quantification of the damage data (such as loosening a bolt not 100% but with a percentage of 77). Therefore, it is prominent to distinguish between two indications. The **Mean Absolute Error (MAE)** is used as the regression metric:

$$MAE = \frac{\sum_{i=1}^n |y_i - x_i|}{n} \quad (4)$$

Where n is the total number of samples, i is the index of sample, y is the predicted value, and x is the actual value of the sample. MAE metric is also used for many regression and classification tasks in both ML and DL studies. For the classification metrics, **Classification Accuracy (CA)** and **Average Precision (AP)** scores are utilized. The CA is one of the most used metrics in ML and DL studies that simply measures the total correct predictions over total predictions:

$$Classification\ Accuracy = \frac{Number\ of\ correct\ predictions}{Total\ number\ of\ predictions} \quad (5)$$

In order to use the CA, a threshold has to be assigned in the domain of prediction scores to convert prediction score into closest label (in this study the used labels are “0” undamaged and “1” damaged). This study used 0.49 as the threshold. The prediction scores made above 0.49 are converted to 1 and the others are to 0. Yet, evaluating a model based on one threshold value can be misleading about the performance of the model. The AP score is one of the most used metric which gives average precision at all possible thresholds, especially employed for benchmarking different DL models on various datasets. It is a very useful metric to compare different models’ successes without specifying a decision threshold. The AP summarizes the precision and recall curve into a one value which represents the weighted summation of precisions at different threshold. The weight is defined as the increase in recall from each succeeding threshold. The precision is the ratio of true positive over sum of true positive and false positive. This metric implies the frequency of correct predictions at every prediction; thus, it reflects how reliable the model is in predicting the samples as positive. Recall is the ratio of true positive over sum of true positive and false negative which implies the model’s ability to classify positive samples and only interests in how the positive samples are classified. The AP can be shown as:

$$AP = \sum_n [Recall(n) - Recall(n - 1)] \times Precision(n) \quad (6)$$

Briefly, the AP is the area under precision-recall curve. An area of 1.0 means that the classifier is a perfect model and 0.5 means the classifier is a poor model.

After M_2 made the predictions on the unseen (test) dataset which each scenario consists of 30 samples as given in Fig. 2, the results including the ground truths and prediction scores are bar plotted in Fig. 12. Also, the **MAE**, **CA**, and **AP** metrics are computed and displayed on the top right corner of the bar plots for each scenario in Figs. 12-17. At first glance, one can catch the close prediction scores to ground truths (actual labels) in these figures. Yet with a closer look, there are few incorrect prediction results. Starting with Scenario#0, the regression and classification metrics show that model predicts with 100% CA, 1.00 AP, and 4.7×10^{-3} MAE. That means model yields consistent results on every tensor with no inaccurate classification. Note that Scenario#0 (no synthetic tensor is involved in) was created as a “reference” scenario for benchmarking purposes. For the rest of the scenarios, from Scenario#1 to Scenario#5, the inclusion ratio of number of synthetic tensors in the damage test dataset are gradually decreased. This change slightly impacted the classification results. Firstly, the corresponding scenarios in Figs. 13-17 includes one incorrect prediction on different tensors that are circled in red color. While the M_2 is more confident on its predictions in

Scenario#1-2-3, for the Scenario#4-5 it remains uncertain on few tensors. The incorrect predictions caused the MAE metric to increase about 6.5 times from 4.7×10^{-3} to 0.3×10^{-1} ranges when comparing **the Scenario#0 to other scenarios**. This indicates that the predictions of M_2 include more errors for the other scenarios than the reference scenario. Having one incorrect prediction caused the CA score decreased from 100% to 97%, while the AP score is decreased from 1.00 to 0.97 only for Scenario#1-2. The change in AP score is basically the result of high confidence of the model on the data for Scenario#1-2. Since the model is very sure of its predictions, the AP score always contains one incorrect prediction at every threshold value unless threshold is selected very close to 0 or 1. While the inclusion of synthetic tensors slightly changed the MAE metric, the CA and AP metrics experienced negligible amount of decreases which is critical for the vibration-based damage detection. The classification metric is more used for the level-1 damage diagnostics (damage detection) and the error metrics can be more beneficial for the level-2 damage diagnostics (damage quantification) since the damage quantification is carried out based on the errors. Hence, considering one incorrect prediction out of 30 predictions for the Scenario#1-2-3-4-5, the prediction results on the test dataset can be concluded as excellent.

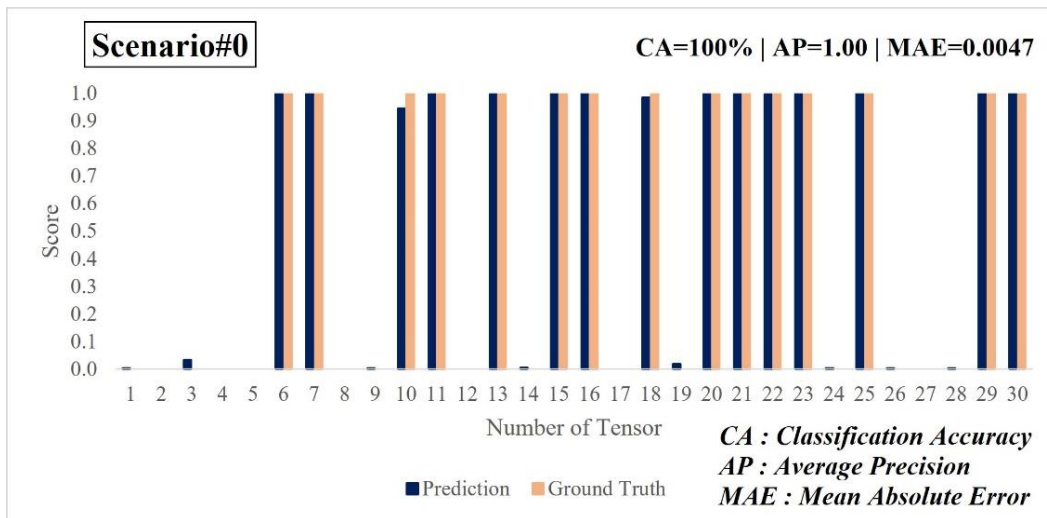


Fig. 12. Testing results of M_2 for Scenario#0

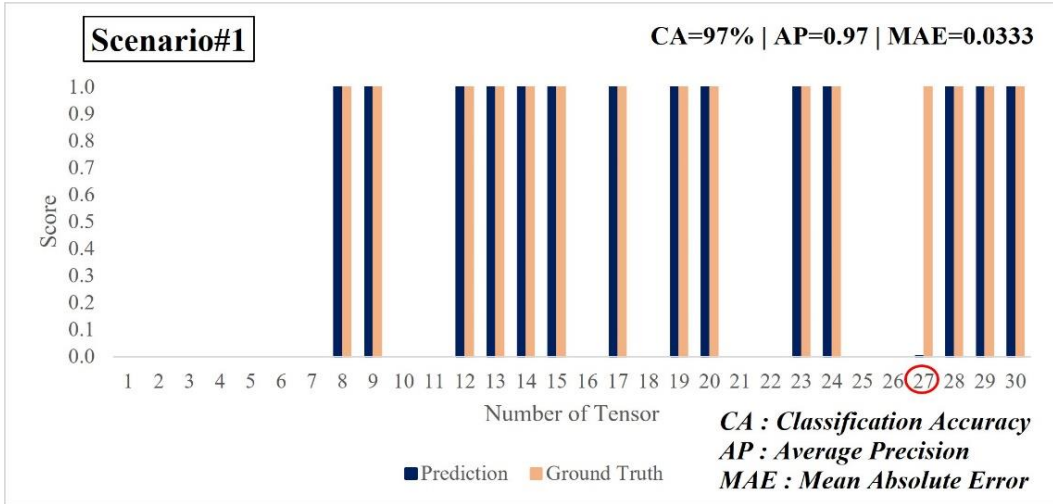


Fig. 13. Testing results of M_2 for Scenario#1

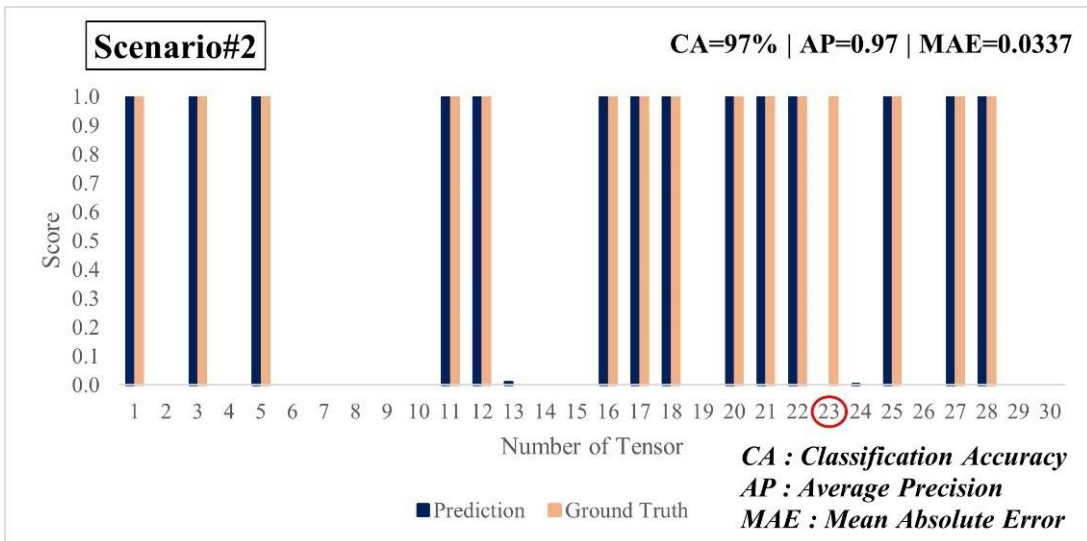


Fig. 14. Testing results of M_2 for Scenario#2

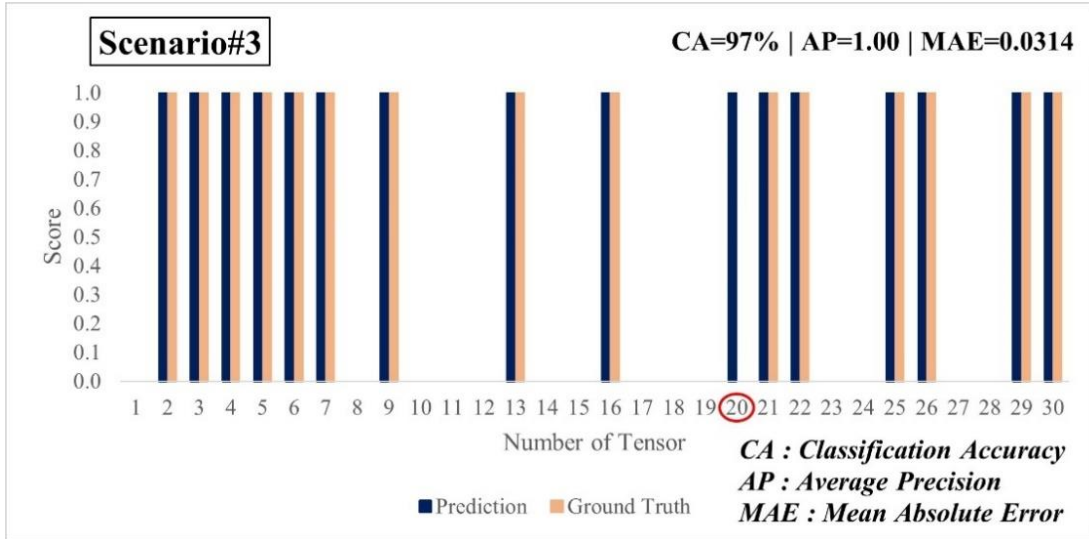


Fig. 15. Testing results of M_2 for Scenario#3

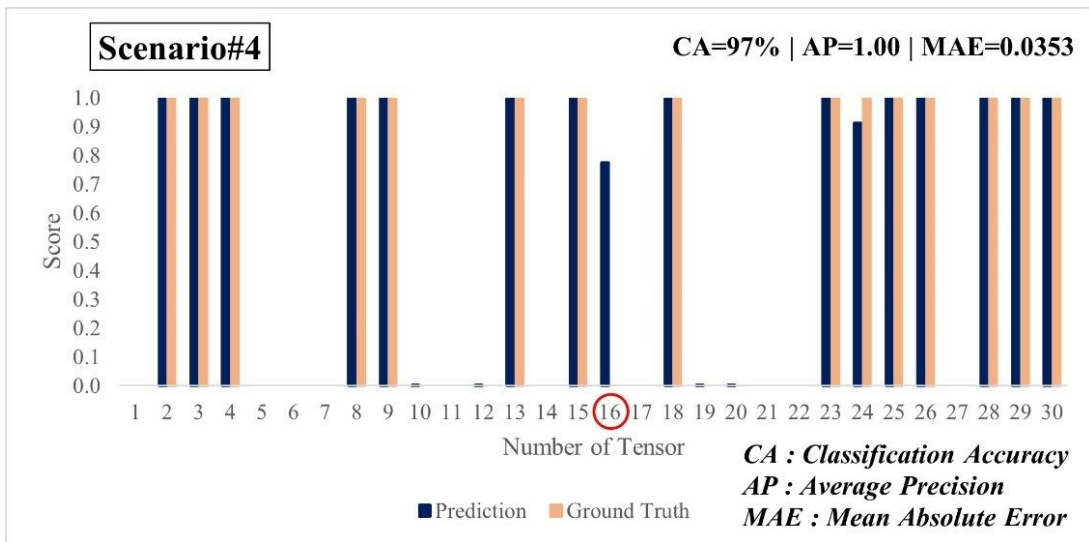


Fig. 16. Testing results of M_2 for Scenario#4

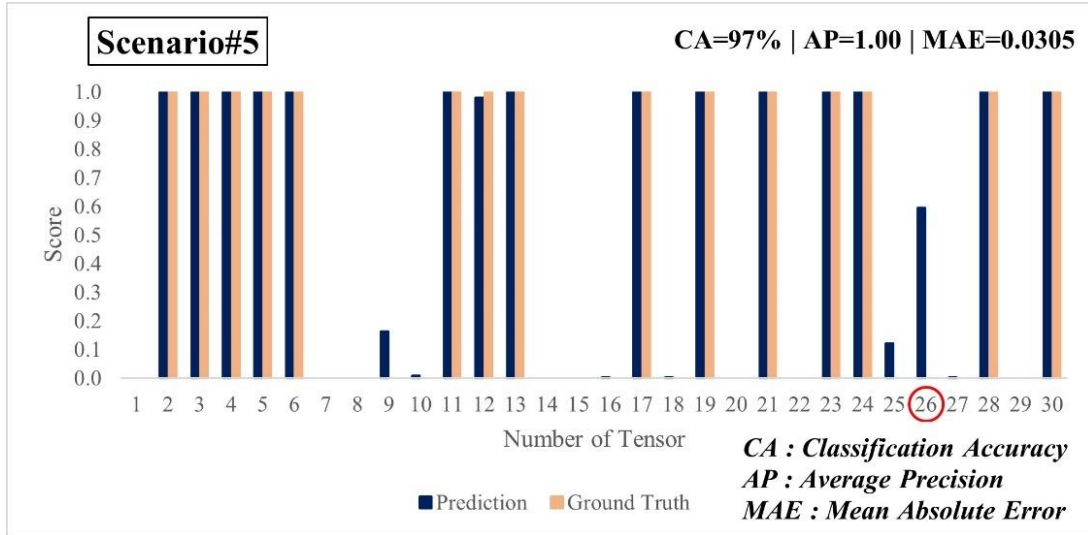


Fig. 17. Testing results of M_2 for Scenario#5

5) Summary and conclusions

Damage diagnostics on civil structures can be very expensive and time consuming because, obtaining vibration dataset that has damage features is challenging. Scarcity of data hinders the use of state-of-the-art data science methods. Recently, the researchers took advantage of such tools such as ML and DL algorithms for vibration-based structural damage diagnostics and they produced excellent results. Particularly the DL methods perform exceptionally well yet it requires large amount of data to operate. This study utilized **One Dimensional Wasserstein Deep Convolutional Generative Adversarial Networks using Gradient Penalty (1-D WDCGAN-GP)** to generate synthetic vibration data and validated the generated datasets with quantitative and qualitative methods. Then, six different scenarios are created to reflect the real-life scenarios that can be faced in SHM of a structure for the purpose of vibration-based damage diagnostics. Each of these scenarios include different levels (ratios) of synthetic vibration tensors mixed with real vibration tensors in the training dataset. Then, for each scenario, 1-D DCNN model is employed to perform damage detection. The 1-D DCNN is trained on the varying ratios of synthetically enhanced training dataset; then tested on the unseen real dataset. The prediction results are evaluated with regression and classification metrics. While the prediction scores for the synthetically enhanced dataset scenarios yielded **97% classification accuracy**, for the real dataset yielded **100% classification accuracy**. The main conclusions of this study can be listed as the following:

- GANs can be used to tackle the imbalanced data due to data scarcity in SHM of civil structures which is a well-known problem in the field. Imbalanced data can be detrimental to ML and DL based damage diagnostic applications. By generating new synthetic datasets with GAN, the training dataset can be balanced. Hence, presented work demonstrated that 1-D WDCGAN-GP can generate very similar vibration data which is indistinguishable from the real ones. Consequently, the proposed methodology and framework in this study paves the way for implementation of additional ML and DL tools to be used in vibration-based structural damage diagnostics for civil structures.
- The outputs of 1-D WDCGAN model is evaluated as they are not a copy of the input nor a copy of other generated datasets which makes the generated outputs more creative and diverse. The reasoning behind this is that the trained model learns the variation range of the real dataset and consequently it is able to add different combination of meanings from the learned range. This is also a similar analogy to the real civil structures where collected dynamic responses from structures consist of similar features in the dataset, but they are not exact copies for the undamaged and damage scenarios. Thus, 1-D WDCGAN can be used successfully to complete a portion of the missing vibration data or completely create new datasets by generating similar “enough” samples to the real data.
- Although this paper used a state-of-the-art GAN, the training procedure of 1-D WDCGAN-GP is still tedious.
- Additional research is needed for level-1 damage diagnostics (detection) and level-2 damage diagnostics (quantification) using GANs. Since, the damage detection is based on classification metrics and damage quantification is based on error metrics, new studies should investigate the effect of GANs on the precision of quantification of structural damages.

Data availability statement

Vibration data used in this study was made available in Abdeljaber et al., 2017. Some or all used models, codes, and detailed results are available from the corresponding author of this paper upon request.

Acknowledgement

The authors would like to thank members of CITRS (Civil Infrastructure Technologies for Resilience and Safety) Research Initiative at the University of Central Florida. The second author would like to acknowledge the support by National Aeronautics and Space Administration (NASA) Award No. 80NSSC20K0326.

Nomenclature

The following symbols are used in this paper:

Symbol	Description
$[a_{01}]_r$	Vibration data at joint#1 in undamaged scenario (0) in raw form (262,144 samples)
$[a_{11}]_r$	Vibration data at joint#1 in damaged scenario (1) in raw form (262,144 samples)
$[a_{11}]_b$	Vibration tensor at joint#1 in damaged scenario (1) in batched form (1024 samples)
$[a_{01}]_b$	Vibration tensor at joint#1 in undamaged scenario (0) in batched form (1024 samples)
$[a_{11f}]_b$	Generated, “fake”, vibration tensor from GAN which the model is trained on $[a_{11}]_r$
M_1	Used 1-D WDCGAN-GP model in the paper
M_2	Used 1-D DCNN model in the paper

References

- Abdeljaber, O. and Avci, O., Nonparametric Structural Damage Detection Algorithm for Ambient Vibration Response: Utilizing Artificial Neural Networks and Self-Organizing Maps, *Journal of Architectural Engineering*, vol. **22**, no. 2, June 2016. DOI: 10.1061/(ASCE)AE.1943-5568.0000205
- Abdeljaber, O., Avci, O., Kiranyaz, M. S., Boashash, B., Sodano, H. and Inman, D. J., 1-D CNNs for Structural Damage Detection: Verification on a Structural Health Monitoring Benchmark Data, *Neurocomputing*, vol. **275**, January 2018. DOI: 10.1016/j.neucom.2017.09.069

- Abdeljaber, O., Avci, O., Kiranyaz, S., Gabbouj, M. and Inman, D. J., Real-Time Vibration-Based Structural Damage Detection Using One-Dimensional Convolutional Neural Networks, *Journal of Sound and Vibration*, vol. **388**, February 2017. DOI: 10.1016/j.jsv.2016.10.043
- Alom, M. Z., Taha, T. M., Yakopcic, C., Westberg, S., Sidike, P., Nasrin, M. S., Hasan, M., Essen, B. C. van, Awwal, A. A. S. and Asari, V. K., A State-of-the-Art Survey on Deep Learning Theory and Architectures, *Electronics*, vol. **8**, no. 3, March 5, 2019. DOI: 10.3390/electronics8030292
- Arjovsky, M., Chintala, S. and Bottou, L., Wasserstein GAN, January 26, 2017.
- Avci, O., Abdeljaber, O., Kiranyaz, S., Hussein, M., Gabbouj, M. and Inman, D., A New Benchmark Problem for Structural Damage Detection: Bolt Loosening Tests on a Large-Scale Laboratory Structure, pp. 15–22, 2022.
- Avci, O., Abdeljaber, O., Kiranyaz, S., Hussein, M., Gabbouj, M. and Inman, D. J., A Review of Vibration-Based Damage Detection in Civil Structures: From Traditional Methods to Machine Learning and Deep Learning Applications, *Mechanical Systems and Signal Processing*, vol. **147**, p. 107077, accessed October 12, 2021, January 15, 2021. DOI: 10.1016/J.YMSSP.2020.107077
- Avci, O., Abdeljaber, O., Kiranyaz, S. and Inman, D., Structural Damage Detection in Real Time: Implementation of 1D Convolutional Neural Networks for SHM Applications, 2017.
- Bandara, R. P., Chan, T. H. and Thambiratnam, D. P., Structural Damage Detection Method Using Frequency Response Functions, *Structural Health Monitoring*, vol. **13**, no. 4, July 19, 2014. DOI: 10.1177/1475921714522847
- Borji, A., Pros and Cons of GAN Evaluation Measures, February 9, 2018.

- Costa, V., Lourenço, N., Correia, J., and Machado, P., COEGAN, *Proceedings of the Genetic and Evolutionary Computation Conference*, New York, NY, USA: ACM, 2019.
- Cury, A. and Crémona, C., Pattern Recognition of Structural Behaviors Based on Learning Algorithms and Symbolic Data Concepts, *Structural Control and Health Monitoring*, vol. **19**, no. 2, March 2012. DOI: 10.1002/stc.412
- Das, S., Saha, P. and Patro, S. K., Vibration-Based Damage Detection Techniques Used for Health Monitoring of Structures: A Review, *Journal of Civil Structural Health Monitoring*, vol. **6**, no. 3, July 9, 2016. DOI: 10.1007/s13349-016-0168-5
- Dong, C.-Z. and Catbas, F. N., A Review of Computer Vision–Based Structural Health Monitoring at Local and Global Levels, *Structural Health Monitoring*, vol. **20**, no. 2, March 20, 2021. DOI: 10.1177/1475921720935585
- Eren, L., Bearing Fault Detection by One-Dimensional Convolutional Neural Networks, *Mathematical Problems in Engineering*, vol. **2017**, 2017. DOI: 10.1155/2017/8617315
- Fan, G., Li, J., Hao, H. and Xin, Y., Data Driven Structural Dynamic Response Reconstruction Using Segment Based Generative Adversarial Networks, *Engineering Structures*, vol. **234**, May 2021. DOI: 10.1016/j.engstruct.2021.111970
- Gao, S., Wang, X., Miao, X., Su, C. and Li, Y., ASM1D-GAN: An Intelligent Fault Diagnosis Method Based on Assembled 1D Convolutional Neural Network and Generative Adversarial Networks, *Journal of Signal Processing Systems*, vol. **91**, no. 10, October 3, 2019. DOI: 10.1007/s11265-019-01463-8
- Gardner, P., and Barthorpe, R. J., On Current Trends in Forward Model-Driven SHM, *Structural Health Monitoring 2019*, Lancaster, PA: DEStech Publications, Inc., 2019.

- Ghiasi, R., Torkzadeh, P. and Noori, M., A Machine-Learning Approach for Structural Damage Detection Using Least Square Support Vector Machine Based on a New Combinational Kernel Function, *Structural Health Monitoring*, vol. **15**, no. 3, May 11, 2016. DOI: 10.1177/1475921716639587
- González, M. P. and Zapico, J. L., Seismic Damage Identification in Buildings Using Neural Networks and Modal Data, *Computers & Structures*, vol. **86**, no. 3–5, February 2008. DOI: 10.1016/j.compstruc.2007.02.021
- Goodfellow, I., NIPS 2016 Tutorial: Generative Adversarial Networks, December 31, 2016.
- Goodfellow, I. J., Pouget-Abadie, J., Mirza, M., Xu, B., Warde-Farley, D., Ozair, S., Courville, A. and Bengio, Y., Generative Adversarial Networks, June 10, 2014.
- Guan, S. and Loew, M., A Novel Measure to Evaluate Generative Adversarial Networks Based on Direct Analysis of Generated Images, February 27, 2020.
- Guan, S., and Loew, M., Evaluation of Generative Adversarial Network Performance Based on Direct Analysis of Generated Images, *2019 IEEE Applied Imagery Pattern Recognition Workshop (AIPR)*, IEEE, pp. 1–5, 2019.
- Gul, M. and Catbas, F. N., Ambient Vibration Data Analysis for Structural Identification and Global Condition Assessment, *Journal of Engineering Mechanics*, vol. **134**, no. 8, August 2008. DOI: 10.1061/(ASCE)0733-9399(2008)134:8(650)
- Gul, M. and Catbas, F. N., Damage Assessment with Ambient Vibration Data Using a Novel Time Series Analysis Methodology, *Journal of Structural Engineering*, vol. **137**, no. 12, December 2011. DOI: 10.1061/(ASCE)ST.1943-541X.0000366

- Gulrajani, I., Ahmed, F., Arjovsky, M., Dumoulin, V. and Courville, A., Improved Training of Wasserstein GANs, March 31, 2017.
- Guo, Q., Li, Y., Song, Y., Wang, D. and Chen, W., Intelligent Fault Diagnosis Method Based on Full 1-D Convolutional Generative Adversarial Network, *IEEE Transactions on Industrial Informatics*, vol. **16**, no. 3, March 2020. DOI: 10.1109/TII.2019.2934901
- Heusel, M., Ramsauer, H., Unterthiner, T., Nessler, B. and Hochreiter, S., GANs Trained by a Two Time-Scale Update Rule Converge to a Local Nash Equilibrium, June 26, 2017.
- Jiang, H., Wan, C., Yang, K., Ding, Y. and Xue, S., Continuous Missing Data Imputation with Incomplete Dataset by Generative Adversarial Networks–Based Unsupervised Learning for Long-Term Bridge Health Monitoring, *Structural Health Monitoring*, June 4, 2021. DOI: 10.1177/14759217211021942
- Krishnan Nair, K. and Kiremidjian, A. S., Time Series Based Structural Damage Detection Algorithm Using Gaussian Mixtures Modeling, *Journal of Dynamic Systems, Measurement, and Control*, vol. **129**, no. 3, May 1, 2007. DOI: 10.1115/1.2718241
- Kuo, P.-H., Lin, S.-T. and Hu, J., DNAE-GAN: Noise-Free Acoustic Signal Generator by Integrating Autoencoder and Generative Adversarial Network, *International Journal of Distributed Sensor Networks*, vol. **16**, no. 5, May 20, 2020. DOI: 10.1177/1550147720923529
- Lee, J. J., Lee, J. W., Yi, J. H., Yun, C. B. and Jung, H. Y., Neural Networks-Based Damage Detection for Bridges Considering Errors in Baseline Finite Element Models, *Journal of Sound and Vibration*, vol. **280**, no. 3–5, February 2005. DOI: 10.1016/j.jsv.2004.01.003
- Lee, J. and Kim, S., Structural Damage Detection in the Frequency Domain Using Neural Networks, *Journal of Intelligent Material Systems and Structures*, vol. **18**, no. 8, August 29, 2007. DOI: 10.1177/1045389X06073640

Luo, T., Fan, Y., Chen, L., Guo, G. and Zhou, C., EEG Signal Reconstruction Using a Generative Adversarial Network With Wasserstein Distance and Temporal-Spatial-Frequency Loss, *Frontiers in Neuroinformatics*, vol. **14**, April 30, 2020. DOI: 10.3389/fninf.2020.00015

MITCSAIL, Spatial Evolutionary Generative Adversarial Networks, <https://jamaltoutouh.github.io/downloads/GECCO-2019-Mustangs.pdf>, 2019.

Pathirage, C. S. N., Li, J., Li, L., Hao, H., Liu, W. and Ni, P., Structural Damage Identification Based on Autoencoder Neural Networks and Deep Learning, *Engineering Structures*, vol. **172**, October 2018. DOI: 10.1016/j.engstruct.2018.05.109

Radford, A., Metz, L. and Chintala, S., Unsupervised Representation Learning with Deep Convolutional Generative Adversarial Networks, November 19, 2015.

Rastin, Z., Ghodrati Amiri, G. and Darvishan, E., Unsupervised Structural Damage Detection Technique Based on a Deep Convolutional Autoencoder, *Shock and Vibration*, vol. **2021**, April 23, 2021. DOI: 10.1155/2021/6658575

Sabir, R., Rosato, D., Hartmann, S., and Guhmann, C., Signal Generation Using 1d Deep Convolutional Generative Adversarial Networks for Fault Diagnosis of Electrical Machines, *2020 25th International Conference on Pattern Recognition (ICPR)*, IEEE, 2021.

Salimans, T., Goodfellow, I., Zaremba, W., Cheung, V., Radford, A. and Chen, X., Improved Techniques for Training GANs, June 10, 2016.

Santos, A., Figueiredo, E., Silva, M. F. M., Sales, C. S. and Costa, J. C. W. A., Machine Learning Algorithms for Damage Detection: Kernel-Based Approaches, *Journal of Sound and Vibration*, vol. **363**, February 2016. DOI: 10.1016/j.jsv.2015.11.008

- Shang, Z., Sun, L., Xia, Y. and Zhang, W., Vibration-Based Damage Detection for Bridges by Deep Convolutional Denoising Autoencoder, *Structural Health Monitoring*, vol. **20**, no. 4, July 28, 2021. DOI: 10.1177/1475921720942836
- Shao, S., Wang, P. and Yan, R., Generative Adversarial Networks for Data Augmentation in Machine Fault Diagnosis, *Computers in Industry*, vol. **106**, April 2019. DOI: 10.1016/j.compind.2019.01.001
- Silva, M., Santos, A., Figueiredo, E., Santos, R., Sales, C. and Costa, J. C. W. A., A Novel Unsupervised Approach Based on a Genetic Algorithm for Structural Damage Detection in Bridges, *Engineering Applications of Artificial Intelligence*, vol. **52**, June 2016. DOI: 10.1016/j.engappai.2016.03.002
- Truong, T., and Yanushkevich, S., Generative Adversarial Network for Radar Signal Synthesis, *2019 International Joint Conference on Neural Networks (IJCNN)*, IEEE, 2019.
- Wang, T., Trugman, D. and Lin, Y., SeismoGen: Seismic Waveform Synthesis Using GAN With Application to Seismic Data Augmentation, *Journal of Geophysical Research: Solid Earth*, vol. **126**, no. 4, April 16, 2021. DOI: 10.1029/2020JB020077
- Wang, Z., Bovik, A. C., Sheikh, H. R. and Simoncelli, E. P., Image Quality Assessment: From Error Visibility to Structural Similarity, *IEEE Transactions on Image Processing*, vol. **13**, no. 4, April 2004. DOI: 10.1109/TIP.2003.819861
- Wulan, N., Wang, W., Sun, P., Wang, K., Xia, Y. and Zhang, H., Generating Electrocardiogram Signals by Deep Learning, *Neurocomputing*, vol. **404**, September 2020. DOI: 10.1016/j.neucom.2020.04.076
- Yin, T., Lam, H. F., Chow, H. M. and Zhu, H. P., Dynamic Reduction-Based Structural Damage Detection of Transmission Tower Utilizing Ambient Vibration Data, *Engineering Structures*, vol. **31**, no. 9, September 2009. DOI: 10.1016/j.engstruct.2009.03.004

Yu, Y., Wang, C., Gu, X. and Li, J., A Novel Deep Learning-Based Method for Damage Identification of Smart Building Structures, *Structural Health Monitoring*, vol. **18**, no. 1, January 8, 2019. DOI: 10.1177/1475921718804132

Zhang, C., Kuppannagari, S. R., Kannan, R., and Prasanna, V. K., Generative Adversarial Network for Synthetic Time Series Data Generation in Smart Grids, *2018 IEEE International Conference on Communications, Control, and Computing Technologies for Smart Grids (SmartGridComm)*, IEEE, 2018.

Zhang, X., Qin, Y., Yuen, C., Jayasinghe, L. and Liu, X., Time-Series Regeneration with Convolutional Recurrent Generative Adversarial Network for Remaining Useful Life Estimation, January 10, 2021.